

Ray Chaos in a Photonic Crystal – Supplementary Materials

Emmanuel Rousseau and Didier Felbacq
*Laboratoire Charles Coulomb (L2C),
UMR 5221 CNRS-Université de Montpellier,
Montpellier, F-France*

These supplementary materials detail some calculations and some experimental results related to the propagation of light in the photonic billiard. We first justify why we focus only on the rays that are transmitted through the cylinders and justify the geometrical optics approximation. Then we explain the dynamical properties of ray propagation, demonstrate that asymptotically the Lyapunov exponent grows as $\lambda \sim \ln t^*$ where $t^* = T/R$ is the photonic crystal period T divided by the cylinder radius R . Finally we close these supplementary materials by presenting some experimental results demonstrating the exponential sensitivity to the initial conditions.

I. REFLECTED VERSUS REFRACTED RAYS

A. propagation of the energy: a binomial process

We demonstrate here that the trajectory of the energy through the photonic billiard is given with a good accuracy by the dynamics of the rays that are transmitted through cylinders. When considering the diffusive properties of light, one has to wonder about the dynamics of the rays that arrive at a specific point of the photonic crystal. We argue here that the energy arriving at a specific point of the photonic crystal has essentially followed the path of the always-refracted rays.

Reflection/refraction at the cylinders boundaries can be seen as a binomial process. The relevant parameter is the probability to be transmitted or reflected at the cylinder boundary. Rays are transmitted through cylinders with probability $t = 0.96$ or reflected with a probability $r = 0.04$. Of course from one cylinder to another a ray can be either transmitted or reflected. This is independent of the previous step where the ray could have been either transmitted or reflected. Of course, reflection or transmission through the cylinder is also a process independent of the ray trajectory. After n steps, the probability that a ray has performed k transmissions and $(n-k)$ reflections is given by the binomial law:

$$p(k) = C_n^k t^k r^{n-k}$$

where $C_n^k = \frac{n!}{k!(n-k)!}$ is the binomial coefficient. Because of the binomial law, the mean number of transmissions is $n \times t$. Note that as a consequence of the binomial law, this mean number of transmissions is also the most probable events (i.e. $n \times t$ transmissions is the event with the higher probability). To fixed idea, for a ray that perform 20 steps in the photonics crystals, it has been $20 \times 0.96 \sim 19$ times transmitted through the cylinder and 1 time reflected. After 100 steps, the ray has been, on average, transmitted 96 times and reflected 4 times. These numbers show without any ambiguities that transmission through cylinders dominates the trajectory of the energy inside the photonic crystal. Whatever the number of steps is, the probability that a ray is transmitted through the cylinder is $t/r = 24$ more important than the probability to be reflected. Such reasoning is in qualitative accordance with the plot in figure S1 where the propagation of a gaussian beam in the photonic billiard is exactly solved using a multiple scattering approach (see below). The incident gaussian beam is split in different rays that are predominantly transmitted through the cylinders. When a reflection occurs it can be considered as a new initial condition for a ray that is now transmitted through the cylinders. Such processes remains of course valid all along the propagation inside the photonics crystal and is not restricted to the short-time behavior of the light propagation.

Our paper elaborates on the dynamics of the always-refracted rays. The opposite limit is the always-reflected rays (i.e. rays for which their dynamics is given by the Lorentz gas dynamics). We have shown here that those rays contribute marginally to the trajectory of the energy. So with a good accuracy the diffusive properties of light in the photonic billiard are given by our results. Correction terms need to include the contribution of the reflections, the first correcting term including the contribution of one reflection, the second correcting term the contribution of two reflections and so on.

B. Gaussian beam propagation

We have computed the propagation of a laser beam through a sample of 7×7 cylinders of the photonic crystal. The Maxwell equations are exactly solved and the result is presented on Fig:S1. The parameters used in the simulation are:

- optical index $n = 1.5$
- wavelength $\lambda = 500 \text{ nm}$
- cylinders radius $R = 20\lambda$
- photonic crystal period $T = 5R$

This simulation indicates that the laser beam can be modeled by rays, a ray being the path of the light energy. The initial gaussian beam is split into many light rays during propagation. It also indicates that the field distribution is dominated by the transmitted rays as a result of the low optical index of the cylinders.

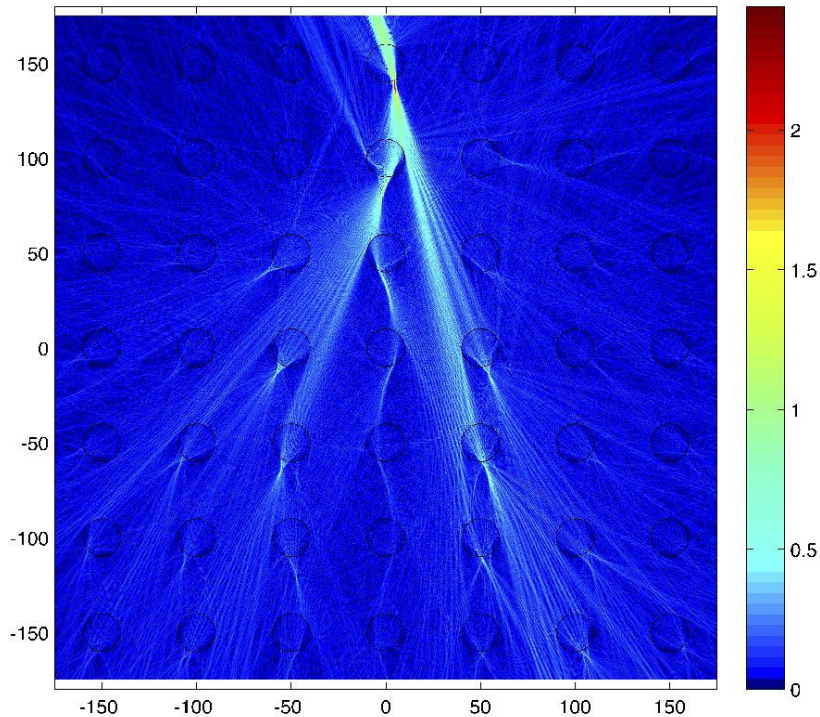


FIG. S1: Propagation of a laser beam into a portion of the photonic crystal.

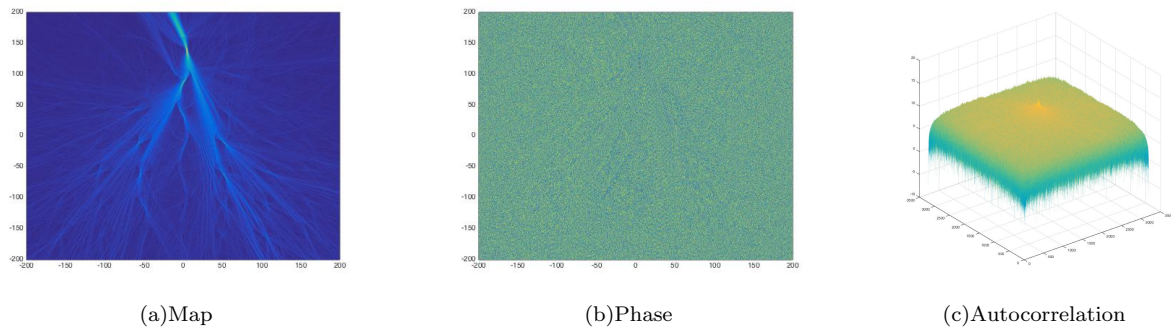
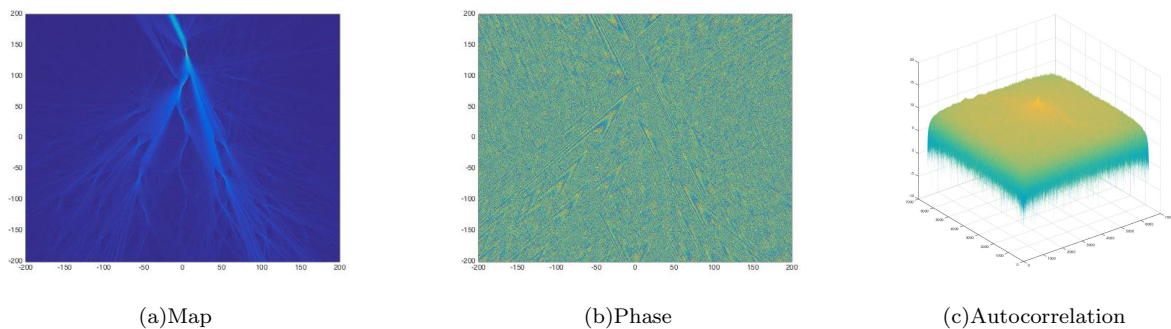
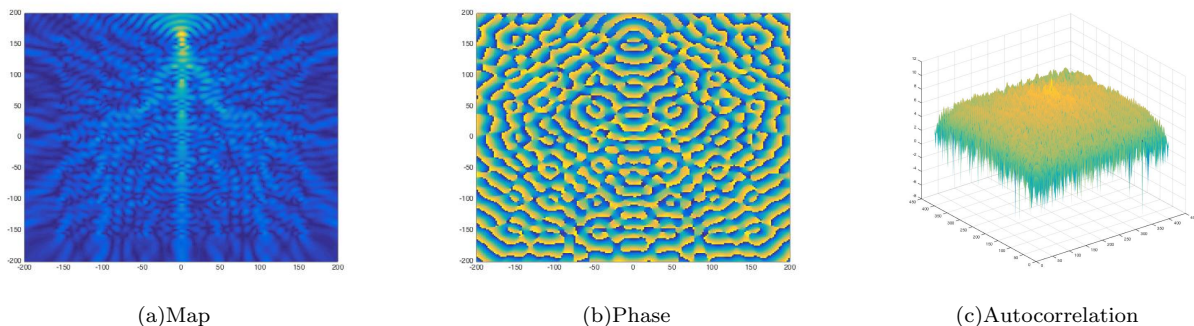
C. Coherence of the waves in the small wavelength regime

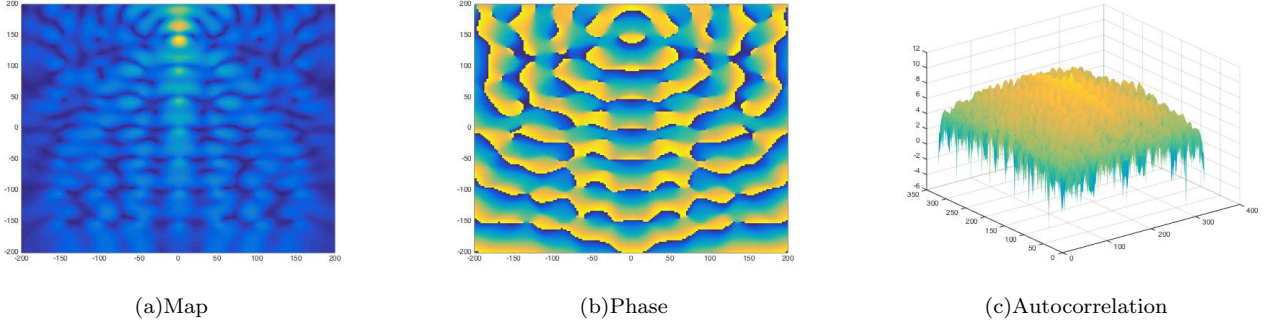
We address here the relevance of the geometrical optics approximation. Given the large number of scattering events, one might wonder whether wave phenomena, i.e. interferences and diffraction might be at stake here. This can be formulated by wondering whether, given a ratio $\eta = \lambda/d$, there is a time t_η (or a number of scattering events N_η) over which "the ray optics approximation" is no longer valid.

As for diffraction, it is certainly true (see e.g. J. Rauch, Hyperbolic systems and geometric optics). However, it is not a problem, because the onset of diffraction simply leads to new rays, described by new initial conditions in phase space : the phase portrait is not modified.

As for interferences, it is another matter. The question is: *after a large number of scattering events, can there be, in the system, a portion of space in which phase coherent phenomena can exist, leading to interferences ?*. Although

this cannot be ruled out (but surely this is certainly difficult to prove rigorously), it seems likely that such phenomena would take place on a scale of a few wavelengths only, that is, in a very small region of space. To sustain this claim, we have performed numerical calculations in which we have solved the complete Maxwell system, for different wavelengths, still much larger than the one used in the experiments (the cylinders are at most $10 \cdot \lambda$ in diameter, while in the experiment they are $10.000 \cdot \lambda$ in diameter : such a size is impossible to deal with numerically when several objects are present, using our available computer power). We have computed the map of the field as well as the map of the phase of the field inside the structure for different wavelength-to-radius ratios : $\lambda/R=5$, $\lambda/R=2$, $\lambda/R=1/2$, $\lambda/R=1/10$. We have also computed the autocorrelation function of the phase. It can be seen (see fig. S2,S3,S4,S5) that already for $\lambda/d=1/10$ the phase is basically a white noise (it is delta-correlated) even after a few scattering events. It is therefore very difficult to believe that a (initially) random field could give rise, after a long time of evolution under the flow of a dynamical system, to coherent phenomena.

FIG. S2: $\lambda/R=1/10$.FIG. S3: $\lambda/R=1/2$.FIG. S4: $\lambda/R=2$.

FIG. S5: $\lambda/R=5$.

II. RAY DYNAMICS

The ray dynamics is split in two part. At the n -step, an incoming ray impinges on a cylinder. It is first refracted at the air/glass interface, then it propagates into the cylinder and finally is refracted at the glass/air interface. This path leads, as seen on Fig:1, to the point B_p . $(\theta_{B_p}, \theta_{B_p}^1)$ can be linked to $(\theta_{A_p}, \theta_{A_p}^1)$ by the set of equations:

$$\theta_{B_p}^1 = -\theta_{A_p}^1 \quad (1)$$

$$\theta_{B_p}^1 = \theta_{A_p} + 2 \arcsin \left(\frac{\sin(\theta_{A_p}^1)}{n} \right) \quad (2)$$

where n is the optical index of the cylinders.

From the point B_p the ray propagates in air until it intersects a new cylinder defining then the point A_{p+1} . The couple $(\theta_{A_{p+1}}, \theta_{A_{p+1}}^1)$ is found with the help of equations:

$$f_B(x) = \tan(\alpha) [x - R \cos(\theta_{B_p})] + R \sin(\theta_{B_p}) \quad (3)$$

$$(x_{A_{p+1}} - x_{p+1}^c)^2 + (f_B(x_{A_{p+1}}) - y_{p+1}^c)^2 = R^2 \quad (4)$$

with α the angle between the horizontal axis and the ray. It satisfies: $\alpha = \theta_{B_p} + \theta_{B_p}^1 = \theta_{A_{p+1}} + \theta_{A_{p+1}}^1$. (x_{p+1}^c, y_{p+1}^c) are the cylinder coordinates at the $(p+1)^{th}$ collision.

The Jacobian J_p of the total transformation $(\theta_{A_p}, \theta_{A_p}^1) \rightarrow (\theta_{A_{p+1}}, \theta_{A_{p+1}}^1)$ is given by $J_p = J_p^{AB} \cdot J_p^{BA'}$ where $J^{BA'}$ is the Jacobian of the transformation $(\theta_{B_p}, \theta_{B_p}^1) \rightarrow (\theta_{A_{p+1}}, \theta_{A_{p+1}}^1)$

$$J_p^{BA'} = \begin{pmatrix} m_n - 1 & m_n \\ 2 - m_p & 1 - m_p \end{pmatrix} \quad (5)$$

with

$$m_p = -\frac{1}{\cos[\theta_{B_p} + \theta_{B_p}^1 - \theta_{A_{p+1}}]} \frac{l_{jump}}{R} \quad (6)$$

where R is the cylinder radius and l_{jump} the distance between the points B_p and A_{p+1} . J^{AB} is the Jacobian of transformation $(\theta_{A_p}, \theta_{A_p}^1) \rightarrow (\theta_{B_p}, \theta_{B_p}^1)$

$$J_p^{AB} = \begin{pmatrix} 1 & \frac{2}{n} \frac{\cos[\theta_{A_p}^1]}{\sqrt{1 - \frac{\sin[\theta_{A_p}^1]}{n}}} \\ 0 & -1 \end{pmatrix} \quad (7)$$

In the Gauss conditions, all Jacobians become independent of n and the Jacobian of the total transformation J reduces to:

$$J_{Gauss} = \begin{pmatrix} \frac{2}{n}t^* + 1 - t^* & 2\left(\frac{n-1}{n}\right) - t^*\left(\frac{n-2}{n}\right) \\ -t^* & 1 - t^* \end{pmatrix} \quad (8)$$

where $t^* = T/R$ is the normalized period of the crystal (T is the crystal period, R is the cylinders radius).

The eigenvalues of the Jacobian in the Gauss conditions are given by:

$$\Lambda_{\pm} = 1 + \frac{t^*}{n} - t^* \pm \frac{1}{n} \sqrt{t^*(n-1)[(n-1)t^* - 2n]} \quad (9)$$

III. PERIOD OF THE BALLISTIC TRAJECTORIES IN THE GAUSS CONDITIONS AND QUASI-PERIODIC TRAJECTORIES;

From Eq:9 it is possible to find the period $P(t^*)$ of the ballistic trajectories in the Gauss conditions. It can be defined as the number of cylinders after which the couple $(\theta_{A_{p+P(t^*)}}, \theta_{A_{p+P(t^*)}^1})$ is equal to $(\theta_{A_p}, \theta_{A_p^1})$. When they are complex numbers, the eigenvalues read:

$$\Lambda_{\pm} = 1 + \frac{t^*}{n} - t^* \pm i \frac{1}{n} \sqrt{t^*(n-1)[2n - (n-1)t^*]}$$

Their modulus is 1 (the map is area preserving). In the eigenbasis the map is given by:

$$\begin{pmatrix} \theta_{A_{p+P(t^*)}} \\ \theta_{A_{p+P(t^*)}^1} \end{pmatrix}_{EB} = \begin{pmatrix} e^{i \arg[\Lambda_+]} & 0 \\ 0 & e^{i \arg[\Lambda_-]} \end{pmatrix}^{P(t^*)} \begin{pmatrix} \theta_{A_p} \\ \theta_{A_p^1} \end{pmatrix}_{EB}$$

where EB refers to the eigenbasis.

Finally we find that the period of the ballistic trajectories in the Gauss conditions is:

$$P(t) = \frac{2\pi}{\arctan\left[\frac{\sqrt{t^*(n-1)[2n - (n-1)t^*]}}{n - t^*(n-1)}\right]} \quad (10)$$

It is plotted in Fig:S6 where we compare numerical results in the Gauss conditions and the analytical formula. We can notice an excellent agreement between the numerical results (green dots in Fig:S6) and the analytical result (plain line in Fig:S6).

The period of the oscillations $P(t^*)$ is a real number whereas the number of cylinders is of course an integer number. This leads to quasi-periodicity. As a matter of fact, in the eigenbasis, for example θ_{A_n} reads $\theta_{A_n} = \theta_{A_0} e^{2i\pi \frac{n}{P(t^*)}}$ where θ_{A_0} is the initial value. If we now write $P(t^*) = I(t^*) - F(t^*)$ where $I(t^*)$ is the nearest integer to $P(t^*)$ and $F(t^*)$ the fractional part. An easy way to understand the origin of quasi-periodicity is to assume that $F(t^*) \ll I(t^*)$. Then we can write $\theta_{A_n} = \theta_{A_0} e^{2i\pi \frac{n}{I(t^*)}} (1 + 2i\pi \frac{nF(t^*)}{I(t^*)^2})$. The first term $e^{2i\pi \frac{n}{I(t^*)}}$ is a periodic function. The second term $(1 + 2i\pi \frac{nF(t^*)}{I(t^*)^2})$ leads to a slipping in the phase space and the trajectory appears as quasi-periodic. It is illustrated by the Fig:S7 for $t^* = 3.2$ and $t^* = 4.2$. The period is $P(3.2) = 3.84$ then $I(3.2) = 4$ and $F(3.2) = 0.16$ and $P(4.2) = 3.17$ with $I(4.2) = 3$ and $F(4.2) = -0.17$. After respectively 4 or 3 steps the point $A_{n+P(t^*)}$ is close to the point A_n but shift from a quantity due to $F(t^*)$ which leads to quasi-periodicity.

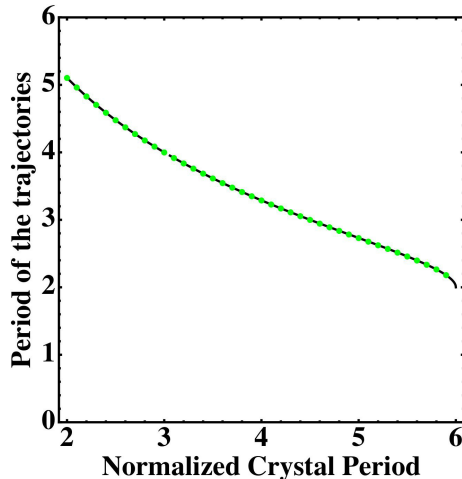


FIG. S6: Period of the ballistic trajectories versus the normalized crystal period $t^* = T/R$. Dots are numerical results whereas the plain line is the analytical result eq.(10).

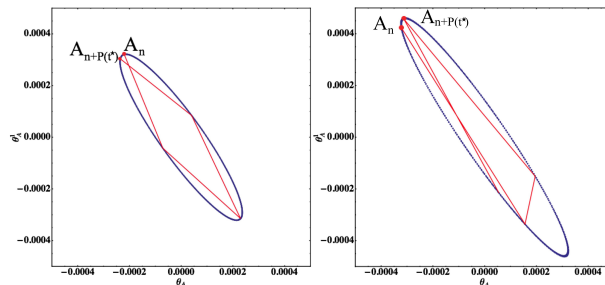


FIG. S7: Phase space for $t^* = 3.2$ and $t^* = 4.2$ in Gauss conditions. Periods are respectively $P(3.2) = 3.84$ and $P(3.2) = 3.17$. This leads to ellipsis in the phase space and quasi-periodicity of the ray trajectory in the crystal.

IV. EXISTENCE OF THE ISLANDS OF STABILITY FOR $t^* < \frac{2n}{n-1}$

Ballistic trajectories in the crystal are characterized by closed curves in phase space (stability islands). Stability islands on their own are characterized by complex eigenvalues of the Jacobian. Thus ballistic trajectories can propagate around the crystal axes ($\theta_A = 0, \pi/2[\pi]$) if $t^* < \frac{2n}{n-1}$ and around the bisectrices ($\theta_A = \pi/4[\pi]$) if $t^* \sqrt{2} < \frac{2n}{n-1}$. This give the threshold above which islands of stability no more exist and above which the motion of light in the crystal is only chaotic.

V. LYAPUNOV EXPONENT BEHAVIOR AT LARGE t^*

Here we show that the Lyapunov exponent grows asymptotically as $\lambda \sim \ln(t^*)$.

For large normalized period of the crystal $t^* \gg 1$ collisions are uncorrelated. So the Jacobian become independent of the step number. Moreover the incident angle θ_A^1 is close to $0[\pi]$. Then J^{AB} reduces to:

$$J^{AB} = \begin{pmatrix} 1 & 0 \\ 0 & -1 \end{pmatrix} \quad (11)$$

and m_n reduces to $m = -\frac{l_j ump}{R}$. The distance between two collisions is given by the mean free path $l_{jump} = \bar{l} = \frac{1}{n^d \sigma} = \frac{(t^*)^2 R}{2}$ where n^d is the density of disks $n^d \sim 1/T^2$ (T is the crystal period) and σ the cross section $\sigma = 2R$.

The Jacobian J of the total transformation $J = J^{AB} \cdot J^{BA'}$ is:

$$J = \begin{pmatrix} m-1 & m \\ m-2 & m-1 \end{pmatrix} \quad (12)$$

The eigenvalues are given by: $\Lambda_{\pm} = \frac{\text{Tr}(J) \pm \sqrt{\text{Tr}(J)^2 - 4}}{2}$. Within the assumption $t^* \gg 1$ the Lyapunov exponent is $\lambda = \ln(\Lambda_+) \sim \ln(t^*)$. So asymptotically it grows as $\ln(t^*)$. Of course the same dependence is found by expanding the positive eigenvalue of the Jacobian Eq:9.

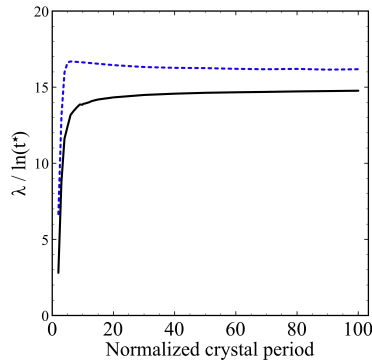


FIG. S8: Lyapunov exponent divided by $\ln(t^*)$ versus the normalized crystal period t^* for the refractive Lorentz gas (plain line) and the reflective Lorentz gas (dashed line).

VI. EXPERIMENTAL RESULTS

We have performed experiments to illustrate that light propagation in the photonic crystal is highly sensitive to the initial conditions. We illuminate a photonic crystal made of 20×20 glass cylinders with a laser beam (cylinder radius ≈ 2 mm, photonic crystal period $T=1.1$ cm leading to $t^* = 2.2$, glass refractive index $n=1.78$, laser wavelength $\lambda=473$ nm). The beam diameter is of the order of 2 mm. It corresponds to a collection of light rays. The dynamics of each of them is described by our model. We start with initial conditions $\theta = 24^\circ$ and $\theta_1 = 24^\circ$. In that case, initial conditions are such that all the laser beam follow a regular path (see Fig: S9)-a). It oscillates with a period close to 4 in agreement with the value given by the equation Eq:10, $P(t^* = 2.2, n = 1.78) = 4.09$. We only increase the incident angle by 3° ($\theta_1 = 37^\circ$). The laser beam starts to follow a regular path (see Fig: S9)-b) but leave the crystal axis and finally diffuse in the entire crystal. By increasing again the initial conditions $\theta_1 = 34^\circ$, the laser beam splits after the first cylinder in several beams that diffuse in the photonic crystal.

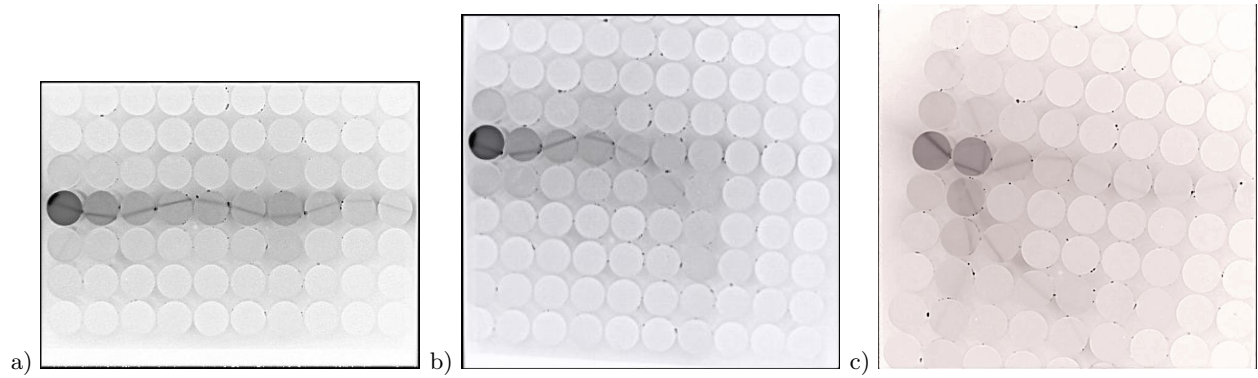


FIG. S9: Experimental results showing propagation of a laser beam in the refractive Lorentz gas. The cylinder radius is $R = 0,5 \text{ cm}$, the crystal period is $T = 1.1 \text{ cm}$ leading to $t = 2.2$. a) The initial conditions are $\theta_0 = 24^\circ$ and $\theta_0^1 = 24^\circ$. The laser beam follows a regular path oscillating back and forth around the crystal axis. b) The initial conditions are $\theta_0 = 24^\circ$ and $\theta_0^1 = 27^\circ$. The laser beam starts to follow a regular path but after hitting 4 cylinders it leaves the crystal axis and diffuses in the entire crystal. c) The initial conditions are $\theta_0 = 24^\circ$ and $\theta_0^1 = 34^\circ$. The laser beam splits in several beams that diffuse in the photonic crystal.